Discover Soil

RESEARCH Open Access

Frequency domain reflectometry and Hydrus-1D for parameterizing the van Genuchten equation in a sandy entisol

Ícaro Vasconcelos do Nascimento[1*], Alexandre dos Santos Queiroz[1], Lucas de Sousa Oliveira[1], João Marcos Rodrigues dos Santos[1], Tiago da Costa Dantas Moniz[1], Raimundo Nonato de Assis Júnior[1], Helon Hébano de Freitas Sousa[1], José Carlos de Araújo[1], Carlos Tadeu dos Santos Dias[1], Cillas Pollicarto da Silva[2], Márcio Godofredo Rocha Lobato[3] and Jaedson Cláudio Anunciato Mota[1]

*Correspondence:
Ícaro Vasconcelos do Nascimento
icaro_agro@hotmail.com
[1]Department of Soil Sciences, Federal University of Ceará, Av. Mister Hull, 2977, Fortaleza 60.021-970, CE, Brazil
[2]Federal Institute of Education, Science and Technology of Piauí, PI 142-Km 02, Pio IX 64660-000, PI, Brasil
[3]Federal Institute of Education, Science and Technology of Piauí, PI 247-Km 07, Uruçuí 64860-00, PI, Brasil

Abstract This study hypothesized that estimating van Genuchten equation parameters using Hydrus-1D, with matric potential data (from tensiometry) and moisture data (from gravimetry and FDR probe), yields soil-water retention curves (SWRC) more consistent with field conditions compared to laboratory methods. The objective was to obtain and compare van Genuchten parameters from Hydrus-1D and laboratory methods. For this, an instantaneous profile experiment was conducted in Fortaleza/CE, Brazil, using four plots (1.5 × 2.0 × 0.5 m) in a loamy sand Entisol. Each plot had an FDR probe access tube (Diviner 2000) and tensiometers (Hg manometer) at depths of 0.2 and 0.4 m. For gravimetric determinations, soil samples were collected at 0.20 and 0.40 m depths concomitantly with tensiometer and FDR readings, and the mass-based water content was converted into volumetric water content using bulk density. When the variation in soil moisture over time reached a threshold drainage rate of $\partial\theta/\partial t = 0.01$ cm^3 cm^{-3} d^{-1}, disturbed and undisturbed samples were collected for lab analysis of bulk density, particle density, porosity, and SWRC, fitted to the van Genuchten model ($m = 1 - [1/n]$). Hydrus-1D estimated four van Genuchten parameters, followed by ANOVA, MANOVA, PCA, and cluster analysis in SAS. Model performance was assessed via efficiency coefficient and RMSE. Results showed that inverse modeling with Hydrus-1D using gravimetry and FDR data yields SWRC better representing field conditions, with FDR probes proving practical and effective for SWRC estimation.

Highlights Hydrus-1D with gravimetry and FDR produced SWRCs consistent with field-derived curves.

FDR probes matched gravimetry performance while reducing labor and time requirements.

Tensiometry captured wet-range dynamics but was less accurate than gravimetry and FDR.

Laboratory-derived curves showed the weakest agreement with field dynamics.

ANOVA, MANOVA, PCA, and cluster analysis confirmed FDR–gravimetry equivalence.

Keywords Soil-water retention curve, Instrumentation in agriculture, Modeling in agriculture, Instantaneous profile, Soil water management

1 Introduction

Given the strong correlation between water management and crop yield, understanding the soil-water retention relationship is of paramount importance in agriculture, as it informs strategies designed to maximize crop yields while minimizing environmental impacts [1, 2]. Moreover, the increasing global demand for food necessitates the development of techniques that enhance water use efficiency in production systems, particularly in marginal soils such as sandy soils.

These soils, which have been incorporated into production systems out of necessity, typically exhibit clay contents lower than 15%, low water retention capacities, limited natural fertility, and are widely distributed globally [3–6]. These challenges are especially critical in sandy soils, where rapid drainage and limited water-holding capacity hinder irrigation efficiency. Recent studies have reinforced the importance of improved methods for characterizing SWRCs in sandy soils [6–9].

Understanding soil moisture is critical for effective water management in agriculture. The gravimetric method, a direct technique, is the most widely used approach for measuring soil moisture; it quantifies the water present in a given mass of soil (or a specific volume, provided that soil density is known) [10]. Alternatively, soil moisture can be determined indirectly through dielectric techniques such as Time Domain Reflectometry (TDR) and Frequency Domain Reflectometry (FDR). TDR estimates soil water content from the travel time of an electromagnetic pulse along a waveguide, whereas FDR probes infer it from the soil's apparent dielectric permittivity at a fixed frequency, detected through changes in the capacitance of an oscillator circuit [11]. FDR devices, which typically consist of a capacitor coupled with an oscillator circuit and a data logger, are generally more portable and practical for routine field use [12, 13].

There exists a direct relationship between matric potential (Ψ_m) and volumetric moisture content (θ), whereby drier soils exhibit more negative Ψ_m values. This relationship is crucial in studies of soil–water retention and can be mathematically expressed as $\theta = f(\Psi_m)$ [14, 15]. The graphical representation of this function is known as the soil–water retention curve (SWRC), which facilitates the evaluation of both available and current water contents in the soil, as well as other essential variables for effective irrigation management [16].

Numerous methods exist for obtaining SWRC, both in the field and the laboratory. A commonly employed technique involves the use of Richards' porous plate apparatus, in which the difference between the sample mass before and after the procedure corresponds to the mass of water in equilibrium with the applied pressure [17].

Given the operational and instrumental challenges associated with determining certain soil hydraulic parameters, such as the SWRC, alternative methodologies have garnered significant attention. One such alternative is inverse modeling [18]. Hydrus-1D [19] exemplifies an inverse modeling approach that estimates soil hydraulic parameters, including the parameters of the van Genuchten (1980) equation [20], and thus the

SWRC. Through an iterative process, the model seeks the optimal solution to Richards' equation, which governs water movement in soils.

The SWRC modeled using Hydrus-1D more accurately represents the soil's hydraulic behavior under field conditions compared to laboratory-derived curves [18]. By incorporating temporal matric potential data into the model, it was concluded that Hydrus-1D reliably estimates the parameters of the van Genuchten equation and, consequently, the soil water potential [21]. Similarly [22], estimated the van Genuchten parameters using gravimetrically obtained moisture data, determined that regardless of soil texture, the SWRC generated by Hydrus-1D aligns more closely with field conditions than those derived in the laboratory.

This study hypothesizes that parameterizing the van Genuchten equation through inverse modeling with Hydrus-1D, using temporal variations of matric potential (tensiometry) and soil moisture (gravimetry and FDR probe), yields SWRCs that better represent field conditions than laboratory-derived curves. In particular, FDR probes are expected to perform as effectively as gravimetry, while offering practical advantages of faster acquisition and reduced labor. Therefore, the objective of this study was to obtain the parameters of the van Genuchten model using Hydrus-1D with temporal data on matric potential (from tensiometry) and moisture (from both gravimetry and FDR probe), alongside laboratory measurements.

2 Materials and methods

2.1 Fieldwork

The experiment was conducted at the Federal University of Ceará (UFC), Pici campus, in Fortaleza/CE, Brazil (546517.24 E, 9586013.83 S - UTM 24 S), in an Entisol of the textural classes loamy sand and sand (Table 1).

The instantaneous profile method was used in four experimental plots with dimensions of 1.5 m x 2.0 m (3.0 m^2) and a drain at 0.5 m depth. The volume of soil was delimited on the sides by masonry walls to avoid lateral subsurface flows [23]. An access tube for the FDR probe was installed in each experimental plot, and, around the tube, at a 0.3 m distance, tensiometers with a mercury manometer were installed at 0.20 and 0.40 m depths (Fig. 1).

Calibration curves for the FDR probe (Diviner 2000) were developed from paired measurements of soil moisture and relative frequency, encompassing the full range of water contents observed in the experiment. Soil samples for calibration were collected with a screw auger at the same depths monitored in the field. Gravimetric water contents were determined from these samples and subsequently converted into volumetric water contents using bulk density values, which were then used to establish the calibration relationship. The average calibration equations for the 0.20 and 0.40 m depths were, respectively, $\theta = 0.5451FR^{3.2274}$ (r^2 = 0.9912) and $\theta = 0.6107FR^{4.8545}$ (r^2 = 0.9919).

Although tensiometers cannot measure approximately 1 bar, in this study, they were used within the wet range of the SWRC (saturation to field capacity), where their

Table 1 Average particle-size of experimental plots

Layer (m)	Sand (%)	Silt (%)	Clay (%)	Textural class
0–0.25	84.1 ± 1.5	8.4 ± 2.4	7.5 ± 3.1	Loamy sand
0.25–0.50	90.7 ± 3.7	6.9 ± 3.3	2.4 ± 0.5	Sand

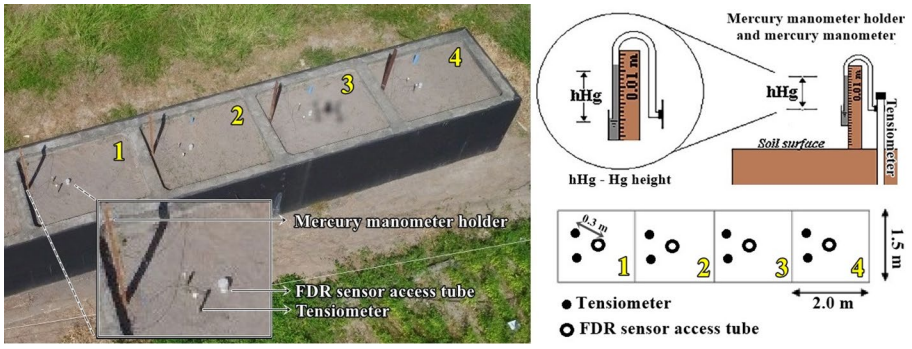

Fig. 1 Aerial view of the experimental plots in field

accuracy is adequate and consistent with the objectives of irrigation-oriented modeling. Tensiometer readings were converted into matric potential (Ψ_m) using Eq. (1).

$$\Psi_m = -12.6h_{Hg} + h_r + z, \tag{1}$$

where h_{Hg} is the height of the Hg column (m), h_r is the height of the *Hg* level in the container with respect to the soil surface (m), and z is the depth of installation considering the center of the tensiometer porous cup (m).

After installing the access tube and tensiometers, each soil column was moistened to ensure saturation. Once the saturation was reached, a plastic tarpaulin was placed on the experimental plot to avoid water flow through the surface, either by evaporation or by infiltration. The time zero ($t = 0$) of water redistribution in the profile was considered to be the moment when the water depth was completely drained from the soil surface.

Concomitantly with the readings of the FDR probe and tensiometers, a soil sample was collected with a screw auger, at each depth mentioned above, with the collection point at a distance of 0.15 to 0.20 m from the tensiometers. In these samples, the moisture content was quantified by the gravimetric method, as follows: each wet sample was weighed and then dried in an oven at a temperature of 105 °C until reaching constant weight. After the process, the samples were weighed again, and the mass difference corresponded to the gravimetric moisture [24].

After the readings with the FDR probe (to obtain volumetric moisture, θ) and tensiometers (to obtain matric potential, Ψm) at t = 0, measurements were taken at 0.17, 0.5, 1, 2, 3, 4, 5, 6, and 7 h, and thereafter every 24 h, until drainage practically ceased. This condition was defined as the point at which the rate of moisture variation with time (∂θ/∂t), calculated from gravimetric data, reached a threshold drainage rate of 0.01 $cm^3\ cm^{-3}\ d^{-1}$, following the criteria adopted in previous inverse modeling studies [18, 21].

Bulk density, which was measured in four replicates, each close to each access tube/tensiometers, was obtained using the Uhland sampler and metal cylinders with dimensions of 0.05 m height and 0.05 m diameter. Volumetric moisture was calculated as the product of gravimetric moisture by bulk density.

2.2 Laboratory determinations

2.2.1 Bulk density

Bulk density was determined from undisturbed cores dried at 105 °C until constant mass [25], which is usually achieved after approximately 24 h, and was calculated as the ratio of the mass of solids to the total volume of soil.

2.2.2 Particle density

Particle density was obtained by the volumetric flask method, whose principle is to determine the volume of alcohol used to complete a 50-mL volumetric flask containing 20 g of oven-dried fine earth [26].

2.2.3 Total porosity

Total porosity was calculated considering bulk density and particle density according to Eq. (2)

$$P = 1 - (\rho_b / \rho_p), \tag{2}$$

where P is the total porosity in $m^3\ m^{-3}$, ρ_p and ρ_b are particles and bulk densities (kg m^{-3}), respectively.

2.2.4 Soil–water retention curve

The soil–water retention curve was determined in undisturbed samples, considering the saturation water content as equal to total porosity. At low tensions (2, 4, 6, 8, and 10 kPa), equilibrium between applied pressure and soil moisture was obtained using a Haines' funnel, whereas for higher tensions (33, 100, 700, and 1500 kPa) it was established with a Richards' porous plate apparatus [27]. In the porous plate system, samples were kept under applied pressure until water drainage through the outlet ceased. The equilibration time was therefore variable depending on the tension, with longer periods required at higher pressures, particularly at 1500 kPa.

2.3 Procedures for obtaining van Genuchten equation parameters

The data obtained in the laboratory were fitted with the program SWRC (*Soil-Water Retention Curve*) [28], considering the model proposed by [20], Eq. 3. The model was fitted by following the Newton-Raphson iterative method, with dependence between m and n [29].

$$\theta = \theta_r + \frac{\theta_s - \theta_r}{[1 + (\alpha\,|\Psi_m|^n)]^m}, \tag{3}$$

where θ corresponds to the water content ($m^3\ m^{-3}$), θ_r and θ_s is, respectively, the residual and saturation water contents ($m^3\ m^{-3}$), Ψ_m is the soil water matric potential (m), α is a scaling factor of Ψ_m (m^{-1}), and m and n are fitting parameters of the model related to the shape.

The second procedure was the inverse modeling with data of matric potentials obtained by tensiometry and moisture (volumetric - θ) obtained by FDR probe and gravimetry. Among the numerous models available to describe SWRC, the model of van Genuchten [29] was used because this equation fits well with the data of a wide variety of soils [30]. With the data of matric potential and moisture over time in the instantaneous profile experiment, Hydrus-1D was used to obtain four parameters of the van Genuchten equation (θ_s, θ_r, α, and n), and the matric potentials and moisture were fitted for each reading time by inverse modeling. The dependence between the parameters m and n, i.e., $m = 1 - (1/n)$ [29] was considered.

In the Hydrus-1D model scenario, the profile of the specimen was divided into two layers, according to the granulometric analysis data and 101 nodes (Fig. 2). Each node is

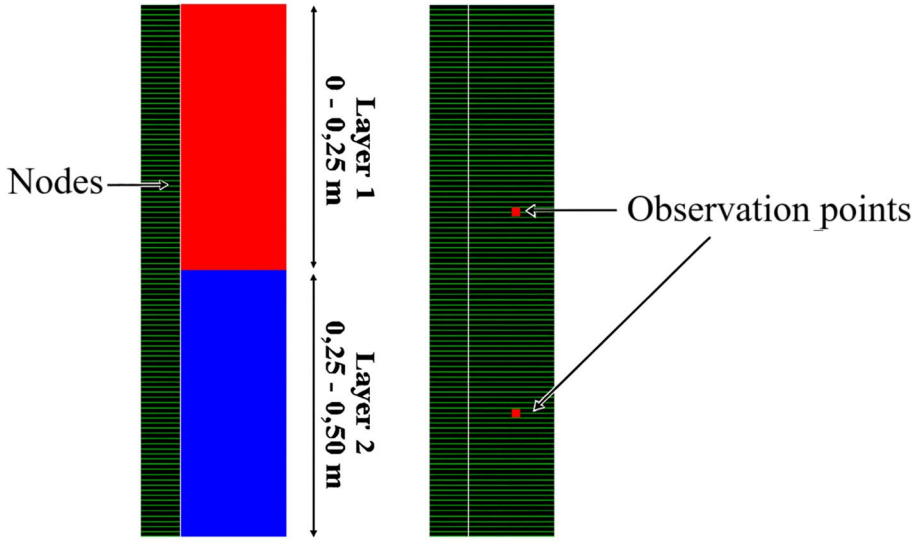

Fig. 2 Profile of the experimental plots in the Hydrus-1D model scenario, showing observation points at 0.20 and 0.40 m depths

a subdivision of the profile and is the target of one iteration, that is, of one data optimization cycle, and appears in green in Fig. 2. Two observation points were considered: 0.2 and 0.4 m, which corresponded to the depths of installation of the tensiometers, readings with the FDR probe, or the sampling depths to obtain moisture content by gravimetry.

The initial values attributed to the hydraulic parameters were θr = 0.1 m^3 m^{-3}, θs = 0.35 m^3 m^{-3}, α = 1 m^{-1}, n = 1.5, K0 = 0.001 m h^{-1}, and l = 0.5 at both depths. These values were chosen as plausible estimates based on typical ranges reported for sandy soils in previous studies and served only as starting points for the inverse optimization process in Hydrus-1D [18, 21, 22]. The tortuosity parameter (l) was fixed at 0.5, as recommended by [20] in the Mualem–van Genuchten model, which is a common assumption in Hydrus-1D applications.

At the soil surface, a zero-flux boundary condition was imposed since a plastic cover eliminated evaporation during drainage. At the lower boundary (0.5 m), a free-drainage condition was defined, corresponding to the drain installed at that depth, which allowed gravitational water flow without impedance. The initial condition of each depth was set with a matric potential of – 0.01 m (practically saturated) for modeling with tensiometry data, whereas in cases using moisture data, the initial condition was set as the moisture at saturation. These assumptions defined the conceptualization of the model and directly influenced the calibration of the soil hydraulic parameters.

The hydraulic parameters were obtained by minimizing the objective function, defined as the sum of the squares of the deviations between observed and simulated values [31]. The objective function was minimized using the Levenberg-Marquardt method [32].

2.4 Statistical data analysis

In the statistical analysis of the data, the methods for obtaining the parameters of the van Genuchten equation, which correspond to the treatments, were termed as shown in Table 2, for both depths.

Table 2 Methods for obtaining the van Genuchten equation parameters and the nomenclature adopted

Depth (m)	Method	Nomenclature
0.20	Laboratory	LAB20
	Gravimetry – HYDRUS 1D	GRAV20
	FDR probe – HYDRUS 1D	FDR20
	Tensiometry – HYDRUS 1D	TEN20
0.40	Laboratory	LAB40
	Gravimetry – HYDRUS 1D	GRAV40
	FDR probe – HYDRUS 1D	FDR40
	Tensiometry – HYDRUS 1D	TEN40

The fitted curves of moisture versus time were plotted to compare the field readings of gravimetric moisture with the values simulated by Hydrus-1D, considering the four procedures for obtaining the parameters of the van Genuchten equation and the two depths. The average soil-water retention curves obtained from field data were also plotted for each depth, using the moisture data obtained by gravimetry and matric potential data obtained by tensiometry, as well as the average soil-water retention curves considering the four methods for obtaining the parameters of the van Genuchten equation. Therefore, the same range of matric potential adopted in the field (matric potential from saturation to field capacity) was considered.

The performance of the model was verified by the following indices: efficiency coefficient – E [33], Eq. 4, and root mean squared error – RMSE, Eq. 5.

$$E = 1 - \frac{\sum_{i=1}^{n} (O_i - P_i)^2}{\sum_{i=1}^{n} (O_i - \bar{O})^2}, \tag{4}$$

$$RMSE = \frac{\sum_{i=1}^{n} (O_i - P_i)^2}{n - 1}, \tag{5}$$

where O_i corresponds to the gravimetric moisture data obtained in the field and P_i corresponds to the moisture data obtained by modeling of soil-water retention curves; n is the number of observations, and $\bar{O}$ is the average of the values obtained in the field. According to [34], the Nash-Sutcliffe efficiency coefficient E can vary from negative infinity to 1, with the unit being the indication of the greatest similarity between data sets [35]. RMSE is used to express the accuracy of the numerical results, showing the error values in the same unit as the measurement of the analyzed variable.

Once the normality of residuals, the absence of outliers, and the homogeneity of variances were verified, an F test (ANOVA) was performed, followed by Tukey's test at the 5% significance level to compare mean values of the van Genuchten parameters (θs, θr, α, m, n). After this univariate analysis, multivariate approaches were applied to provide a more detailed evaluation: multivariate analysis of variance (MANOVA), principal component analysis (PCA), and cluster analysis. MANOVA was used to test whether the joint vectors of means of the van Genuchten parameters differed among methods, based on four alternative statistics: Wilks' Lambda, Pillai's Trace, Hotelling–Lawley Trace, and Roy's Greatest Root. Although each statistic is calculated differently, all test the same null hypothesis of equality between mean vectors. PCA was then applied to condense the van Genuchten parameters into principal components that captured the majority of variance among treatments. This dimensionality reduction highlighted the parameters with the

highest discriminatory power and facilitated visualization of similarities between methods. Complementarily, cluster analysis was used to group treatments according to maximum similarity in their parameter sets. All analyses were conducted on the SAS Studio® platform.

3 Results and discussion

Figure 3A and B illustrate the temporal variation of soil moisture across all scenarios examined in this study for depths of 0.20 and 0.40 m, respectively. Drainage was considered negligible ($\partial\theta/\partial t$ = 0.01 cm^3 cm^{-3} d^{-1}) after 287 h from the initial measurement. Notably, the moisture-time data simulated by Hydrus-1D in treatments GRAV20, FDR20, GRAV40, and FDR40 exhibited strong concordance with field observations, with efficiency coefficients (E) ranging from 0.88 to 0.91 and practically null RMSE values.

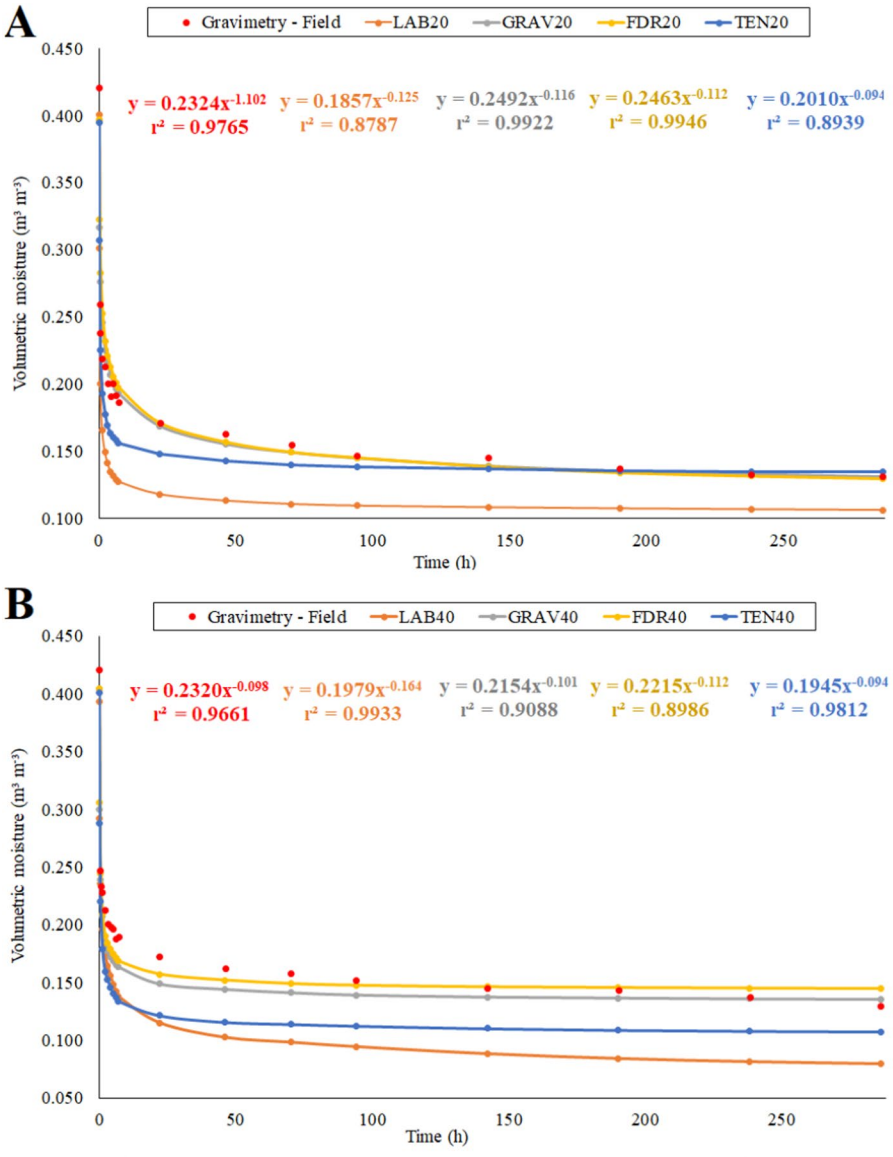

Fig. 3 Temporal variation of volumetric moisture at 0.20 m (**A**) and 0.40 m (**B**). Observed = Gravimetry (red dots); modeled = LAB, GRAV, FDR, TEN. Performance (E; RMSE): 0.20 m—GRAV (0.91; 0.0004), FDR (0.90; 0.0005), TEN (0.55; 0.0007), LAB (0.46; 0.0024). 0.40 m—GRAV (0.88; 0.0005), FDR (0.90; 0.0004), TEN (0.55; 0.0020), LAB (0.43; 0.0025)

The efficiency coefficient (E) is a robust parameter for evaluating the performance of hydrological models, as it quantifies the similarity between modeled and field-measured data [36]. Consequently, the inverse modeling outcomes for these scenarios are consistent with the field's water dynamics, corroborating previous findings [18, 21, 22]. Gravimetry is a direct method, whereas FDR is indirect; however, when properly calibrated, FDR measurements show high concordance with gravimetric values, which explains their comparable performance in inverse modeling.

For both depths, the moisture variation predicted via modeling of tensiometry data (TEN20 and TEN40) showed lower agreement with field observations, with E = 0.55. So, the performance of tensiometry was inferior, since it measures only matric potential (Ψm), which must then be converted into water content (θ) through the fitted SWRC, introducing an additional source of uncertainty [21]. similarly observed strong resemblance between field-measured moisture variations and Hydrus-1D simulations using tensiometry data in sandy soils (>80% sand content). Conversely, the lowest performance was observed in the laboratory-derived SWRCs, with efficiency coefficients of only 0.43–0.46, highlighting their limited representativeness of field water dynamics due to sampling and boundary condition artifacts.

Table 3 presents the mean values of the van Genuchten parameters for each method and depth. Only the curves obtained from inverse modeling with FDR probe data were statistically indistinguishable from those derived from gravimetric data, confirming that both approaches provide equivalent SWRCs [37, 38]. In contrast, tensiometry- and laboratory-derived parameters differed significantly, reflecting their limitations for parameterization.

Among the individual parameters, residual water content (θr) was consistently overestimated by inverse modeling compared to laboratory data. This bias arises because Hydrus-1D was supplied with data from free-drainage experiments that terminate when moisture variation becomes negligible ($\partial\theta/\partial t$ = 0.01 $cm^3\ cm^{-3}\ d^{-1}$ in this study), meaning that calibration is based only on the wet portion of the SWRC (saturation to field capacity). As noted by [18], such restriction limits the model's ability to reproduce the dry end of the curve and may also influence the estimation of α, m, and n, since these parameters are strongly related to curve shape and pore-size distribution [38]. While this limitation is inherent to the methodology, it highlights the need for future studies incorporating a broader moisture range to improve parameter estimation.

Table 3 Mean values of the van Genuchten (1980) parameters at 0.20 and 0.40 m depths, estimated by Hydrus-1D inverse modeling with gravimetry, FDR probe, tensiometry, and laboratory methods

Depth (m)	Parameter	Method			
		GRAV	FDR	TEN	LAB
0.20	θr ($m^3\ m^{-3}$)	0.086 b	0.082 b	0.124 a	0.077 b
	θs ($m^3\ m^{-3}$)	0.400 b	0.400 b	0.408 ab	0.428 a
	α (m^{-1})	4.063 b	3.941 b	5.102 a	4.110 b
	m	0.558 b	0.574 b	0.761 a	0.519 b
	n	2.284 b	2.349 b	4.235 a	2.093 b
0.40	θr ($m^3\ m^{-3}$)	0.128 a	0.138 a	0.100 b	0.034 c
	θs ($m^3\ m^{-3}$)	0.407 a	0.412 a	0.415 a	0.421 a
	α (m^{-1})	3.766 b	4.489 ab	5.250 a	5.022 a
	m	0.774 a	0.800 a	0.779 a	0.676 b
	n	4.502 a	5.000 a	4.532 a	3.130 b

Means followed by the same letter in a row do not differ significantly according to tukey's test at the 5% significance level

Conversely, θs was underestimated, consistent with the fact that field saturation rarely fills all soil pores [39, 40]. In contrast, laboratory samples showed higher θs values due to saturation by capillarity, which fills nearly all pores [41], leading to overestimation compared to field conditions.

Finally, the parameter α, which acts as a scaling factor of Ψm [42], together with m and n, which are related to curve shape and pore-size distribution [18, 20, 38], were statistically indistinguishable between FDR and gravimetry. This reinforces that both approaches adequately describe SWRC geometry and highlights their practical utility for irrigation management in sandy soils.

The multivariate contrasts (Table 4) corroborated these findings, since only FDR- and gravimetry-based curves presented statistically similar mean vectors. In contrast, tensiometry- and laboratory-based scenarios remained significantly different. Tensiometry-based modeling relies on an initial estimation of matric potential variation, which must then be converted into water content using the modeled SWRC; consequently, the reliability of this approach is critically dependent on the quality of SWRC parameterization.

For laboratory-derived curves, the weaker performance is partly explained by sampling and boundary-condition artifacts. Soil sampling for physical analyses, such as SWRC determination, must be carefully planned to ensure field representativeness [43]. Nevertheless, even with optimal sampling, laboratory-imposed boundary conditions differ from those in the field, which can lead to discrepancies in estimated parameters [44]. Together, these results highlight the superior reliability of gravimetry- and FDR-based inverse modeling under field conditions.

The score matrix for the van Genuchten [20] equation parameters, derived from data at both 0.2 and 0.4 m depths and organized along two principal components (PC1 and PC2), are provided in Table 5. For PC1, the variables exhibiting the highest discriminatory power were m (0.60), n (0.59), and θr (0.4646), whereas in PC2, the most influential variables were θs (0.66), α (0.62), and θr (−0.42). Accordingly, PC1 is characterized by curves with high slope and residual moisture (θr), as m and n relate to the SWRC slope;

Table 4 Multivariate contrasts (MANOVA) for soil water retention curves estimated by different methods, based on the joint set of Van Genuchten parameters (θr, θs, α, m, n)

Statistical test	**Contrasts**					
	GRAV20 vs. LAB20	**GRAV20 vs. FDR20**	**GRAV20 vs. TEN20**	**LAB20 vs. FDR20**	**LAB20 vs. TEN20**	**FDR20 vs. TEN20**
	***P*>F**	***P*>F**	***P*>F**	***P*>F**	***P*>F**	***P*>F**
Wilks' Lambda	< 0.0001	0.4252^{ns}	< 0.0001	< 0.0001	< 0.0001	< 0.0001
Pillai's Trace	< 0.0001	0.4252^{ns}	< 0.0001	< 0.0001	< 0.0001	< 0.0001
Hotelling-Lawley Trace	< 0.0001	0.4252^{ns}	< 0.0001	< 0.0001	< 0.0001	< 0.0001
Roy's Greatest Root	< 0.0001	0.4252^{ns}	< 0.0001	< 0.0001	< 0.0001	< 0.0001
Statistical test	**Contrasts**					
	GRAV40 vs. LAB40	**GRAV40 vs. FDR40**	**GRAV40 vs. TEN40**	**LAB40 vs. FDR40**	**LAB40 vs. TEN40**	**FDR40 vs. TEN40**
	P>F	**P>F**	**P>F**	**P>F**	**P>F**	**P>F**
Wilks' Lambda	< 0.0001	0.4252^{ns}	< 0.0001	< 0.0001	< 0.0001	< 0.0001
Pillai's Trace	< 0.0001	0.4252^{ns}	< 0.0001	< 0.0001	< 0.0001	< 0.0001
Hotelling-Lawley Trace	< 0.0001	0.4252^{ns}	< 0.0001	< 0.0001	< 0.0001	< 0.0001
Roy's Greatest Root	< 0.0001	0.4252^{ns}	< 0.0001	< 0.0001	< 0.0001	< 0.0001

Statistics reported: wilks' Lambda, pillai's Trace, Hotelling–Lawley Trace, and roy's greatest root

^{ns} not significant; < 0.0001: Highly significant

Table 5 Matrix of scores for the Van Genuchten (1980) equation parameters, considering the data of both depths (0.2 and 0.4 m), in the two principal components selected (PC1 and PC2)

Variables	PC1	PC2
θr	0.46	−0.42
θs	−0.07	0.66
α	0.27	0.62
m	0.60	0.04
n	0.59	0.08
Eigenvalues	2.70	1.54
Variance (%)	53.98	30.88
Cumulative variance (%)	53.98	84.86

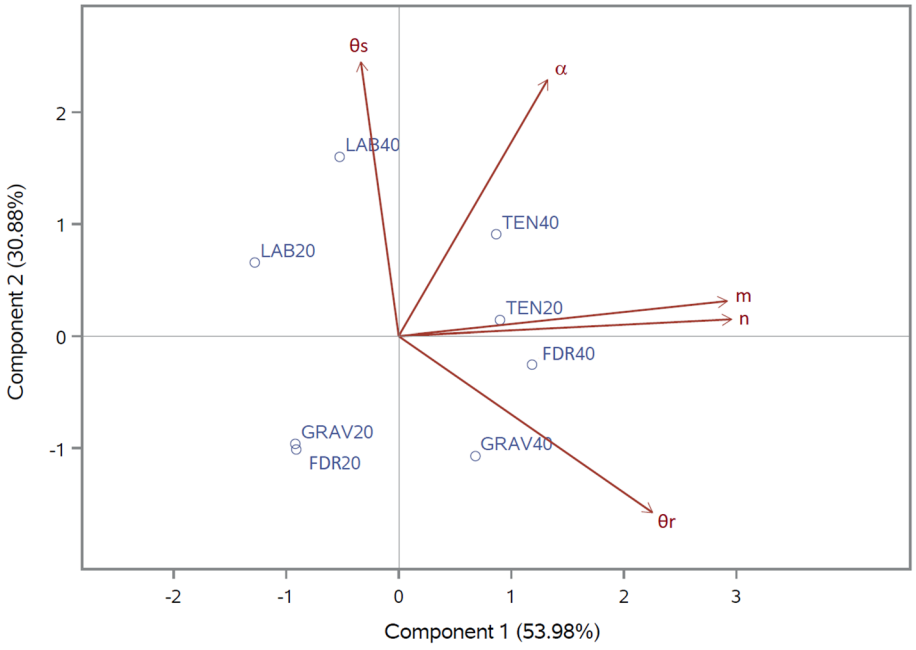

Fig. 4 Biplot chart with the two principal components selected

PC2 is defined by curves with high saturation moisture (θs), similar shape (α), and low residual moisture (θr). Together, these two components explain 84.86% of the data variance (Fig. 4).

Treatments FDR40 and GRAV40 exhibit elevated θr values, in contrast to the laboratory treatments (LAB20 and LAB40), which display below-average θr values (Fig. 4). [13] noted that Hydrus-1D, when supplied with moisture data from free-drainage experiments (terminating when the moisture variation is deemed insignificant, $\partial\theta/\partial t$ = 0.01 $cm^3\ cm^3\ d^{-1}$ in this study), struggles to model the driest portion of the curve due to the data being confined to saturation and field capacity. Nonetheless, since the wet segment of the SWRC is primarily used in irrigation management, the modeled curves remain functionally adequate. High θs values were observed in laboratory samples (LAB20 and LAB40), whereas GRAV40 and FDR40, as well as GRAV20 and FDR20, exhibited below-average saturation moisture values. [39] attribute this discrepancy to the field condition, where soil pores are rarely completely saturated at the time of experimental saturation attempts, unlike the laboratory condition, where capillarity ensures full saturation. [40] reported that field saturation moisture values typically range from 70 to 90%

of soil porosity, thereby corroborating these findings. In the present study, Hydrus-1D estimated saturation moisture at 93–97% of porosity for a 0.20 m depth and 97–99% for a 0.40 m depth.

For the parameter α, Hydrus-1D modeling yielded low values, particularly for GRAV20, FDR20, GRAV40, and FDR40, indicating similar curve shapes among these treatments [22, 38]. Parameters m and n displayed higher values in treatments TEN20 and TEN40, suggesting a more uniform pore distribution and steeper curves. A similar trend was observed for GRAV40 and FDR40, which also recorded values above the mean. These results are consistent with the predominance of macropores in sandy soils, where higher n values correspond to steeper SWRCs [18].

The dendrogram depicted in Fig. 5 delineates the primary clusters identified. The first cluster consists of FDR40 and GRAV40, the second comprises TEN20 and TEN40, the third is formed solely by LAB40, and the fourth group comprises LAB20, FDR20, and GRAV20. The dendrogram reveals a clear grouping trend between SWRCs modeled with gravimetric data and those modeled with FDR probe data, further confirming their equivalence and the divergence of laboratory-based curves. This observation is consistent with the MANOVA results presented in Table 4.

The average field soil-water retention curves for each depth derived from gravimetric moisture data and tensiometry-derived matric potential data are displayed in Fig. 6A and B alongside the average curves from the modeling scenarios. Notably, the lowest agreement was observed between field and laboratory data, which corresponded to the lowest efficiency coefficients (E = 0.4614 for LAB20 and E = 0.4336 for LAB40). This finding reinforces that laboratory-derived curves are less representative of field water redistribution dynamics than those modeled with Hydrus-1D.

Based on the present findings, it is recommended to utilize curves modeled using moisture data obtained by either the gravimetric method or the FDR probe. The FDR probe offers the additional benefit of operational practicality, as it obviates the need for

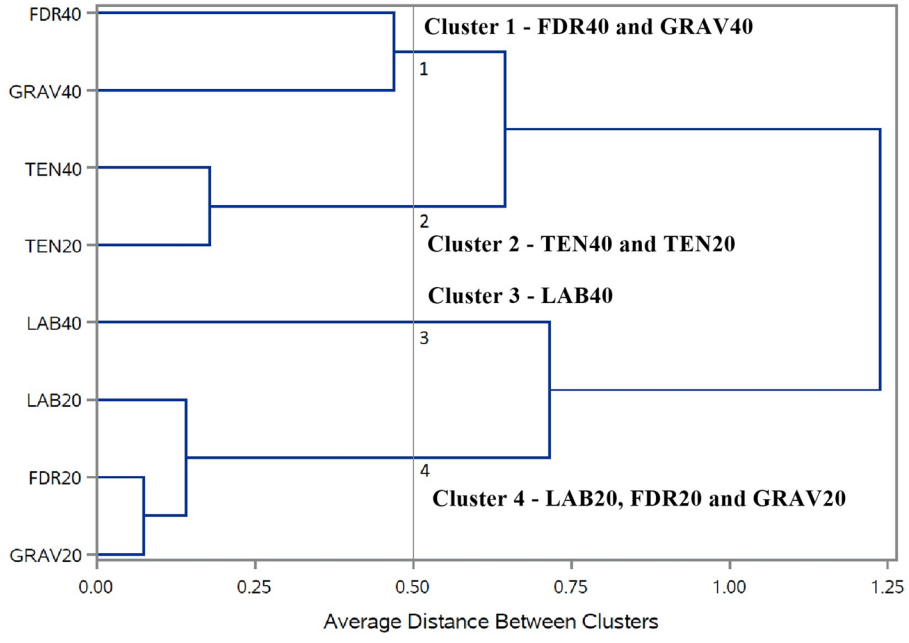

Fig. 5 Dendrogram with the main groups formed

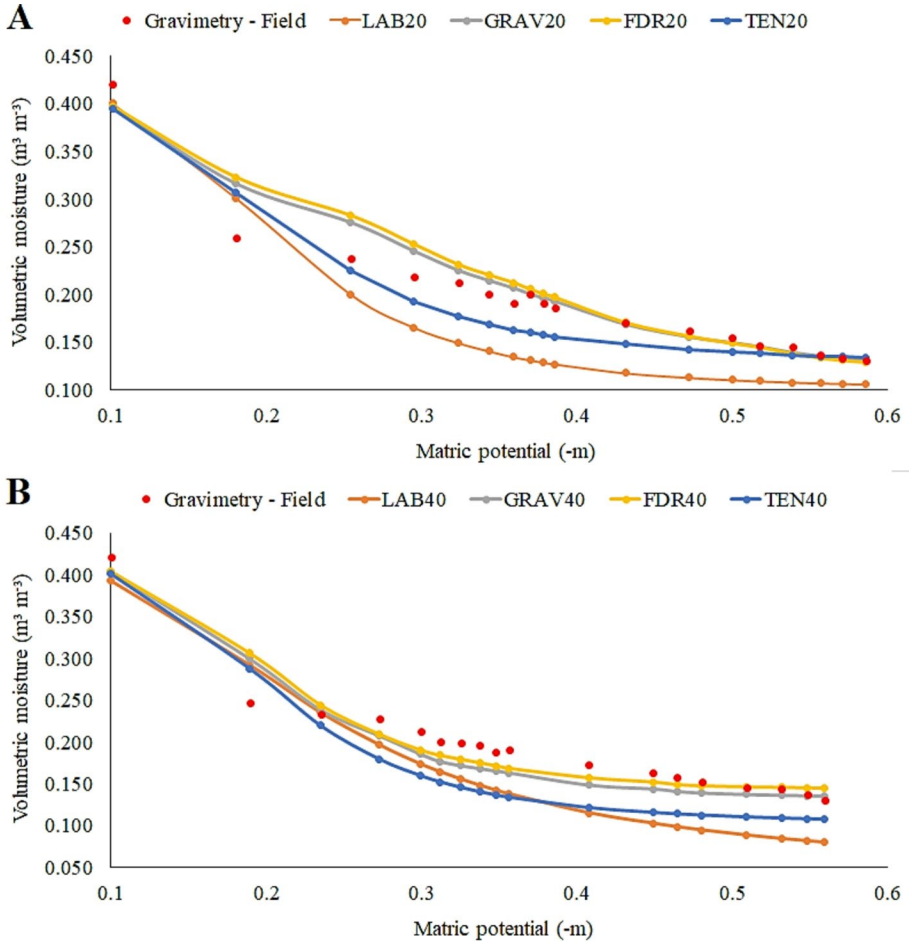

Fig. 6 Soil–water retention curves at depths of 0.20 m (**A**) and 0.40 m (**B**). Gravimetry–Field data (red dots). Modeled curves: Laboratory (LAB20, LAB40), Gravimetry–Hydrus-1D (GRAV20, GRAV40), FDR–Hydrus-1D (FDR20, FDR40), and Tensiometry–Hydrus-1D (TEN20, TEN40)

sample collection and reduces the time required compared to the gravimetric method, which typically necessitates approximately 24 h for oven drying to constant weight. Although the calibration of the FDR probe may be seen as a potential drawback, its accuracy in acquiring soil moisture data is commendable once properly calibrated. However, potential calibration drift and long-term stability must be considered, particularly under variable field conditions. In addition, FDR readings can be influenced by soil salinity, which may affect accuracy in certain environments. These limitations highlight the importance of periodic recalibration and further validation under diverse soil conditions. Thus, employing Hydrus-1D with FDR probe-derived moisture data proves to be both practical and efficient for obtaining reliable SWRCs.

Although the present findings demonstrate the robustness of FDR-based inverse modeling in sandy Entisols, caution is required when extrapolating them to finer-textured soils or soils under saline conditions, where probe calibration and soil–water interactions may differ. FDR probes, while effective once properly calibrated, may be subject to calibration drift and sensitivity to soil salinity, which can affect long-term reliability [45]. These aspects highlight the importance of further testing across different types of soil and climates to validate the broader applicability of this approach.

4 Conclusions

Inverse modeling with Hydrus-1D using gravimetric and FDR probe data resulted in soil-water retention curves that more accurately reflected field conditions compared to laboratory-derived curves.

The FDR probe proved as effective as gravimetry while offering greater practicality, reducing labor requirements, and shortening the time needed to obtain SWRCs. This reinforces its potential as a reliable tool for irrigation management and other field-based hydrological applications.

Although tensiometry was adequate within the wet portion of the SWRC, its predictive capacity was lower than that of gravimetry and FDR, whereas laboratory-derived curves showed the lowest agreement with field dynamics.

Therefore, the use of Hydrus-1D combined with FDR probes is recommended as a practical and efficient alternative for rapid SWRC estimation in sandy soils. Future studies should validate these findings in finer-textured soils and under different environmental conditions, including saline scenarios, to broaden their applicability and to assess the long-term stability of FDR probe calibrations.

Author contributions

I.V.N. conceived the study, conducted the field experiment, performed data tabulation, statistical analysis, prepared the figures, and wrote the manuscript. A.S.Q., L.S.O., J.M.R.S., T.C.D.M., C.P.S., and M.G.R.L. contributed to the field experiment and manuscript writing. R.N.A.J., H.H.F.S., and J.C.A. contributed to supervision and manuscript writing. C.T.S.D. was responsible for statistical analysis, supervision, and manuscript writing. J.C.A.M. contributed to the study conception, field experiment, data tabulation, statistical analysis, figure preparation, and manuscript writing. All authors reviewed and approved the final version of the manuscript.

Funding

A.S. Queiroz, and Í.V. Nascimento express their gratitude to the Federal Agency for Support and Evaluation of Graduate Education (CAPES) for their scholarships. J.M.R.S is grateful to FUNCAP for the scholarship grant under Process no. BMD-0008-01029.01.08/23. J.C.A. Mota acknowledges CNPq (National Council for Scientific and Technological Development) for their research grants (Processes: 303524/2022–7).

Data availability

The datasets generated and analyzed during the current study, including soil moisture and matric potential measurements as well as Hydrus-1D input/output files, are not publicly archived but are available from the corresponding author upon reasonable request.

Declarations

Ethics approval and consent to participate

This study did not involve any human participants or animals. All experimental procedures followed institutional, national, and international guidelines and regulations. No ethical approval was required for this research. Consent to Participate is not applicable.

Consent for publication

All authors have read and approved the final version of the manuscript and consent to its submission and publication in this journal.

Competing interests

The authors declare no competing interests.

Received: 2 June 2025 / Accepted: 26 September 2025

Published online: 13 October 2025

References

1. Hashemi S, Darzi-Naftchali A, Karandish F, Ritzema H, Solaimani K. Enhancing agricultural sustainability with water and crop management strategies in modern irrigation and drainage networks. Agric Water Manag. 2024;305:109110.
2. Liu Y, Song W. Modelling crop yield, water consumption, and water use efficiency for sustainable agroecosystem management. J Clean Prod. 2020;253:119940.
3. Di Raimo LAL, Couto EG, Demattê JAM, Amorim RSS, Torres GN, Cremon C, Mello DC, Bocuti ED, Poppiel RR, Silva AN, Lima LN, Neto LCG. Sand fractions micromorphometry detected by Vis-NIR-MIR and its impact on water retention. Eur J Soil Sci. 2022;73(2). e13227.

4. Yost JL, Hartemink AE. Soil organic carbon in sandy soils: a review. In: Sparks DL, editor. Advances in agronomy. Academic; 2019. pp. 217–310.
5. Osman KT. Sandy soils. In: Osman KT, editor. Management of soil problems. Edinburgh: Springer Nature; 2018. pp. 37–65.
6. Huang J, Hartemink AE. Soil and environmental issues in sandy soils. Earth Sci Rev. 2020;208:103295.
7. Farooq U, Ajmal M, Li S, Yang J, Ullah S. Evaluation of Pedotransfer functions to estimate soil water retention curve: A conceptual review. Water (Basel). 2024;16(17):2547.
8. Zhou J, Ren J, Li Z. An improved prediction method of Soil-Water characteristic curve by geometrical derivation and empirical equation. Math Probl Eng. 2021;2021:1–22.
9. Shokrana MSB, Ghane E. Measurement of soil water characteristic curve using HYPROP2. MethodsX. 2020;7:100840.
10. Dalmago GA, Bergamaschi H. Evaporation of the soil water in response to the amount of straw and evaporative demand. Agrometeoros. 2018;25(2):361–71.
11. Reichardt K, Timm LC. Soil, plant and atmosphere. Cham: Springer International Publishing; 2020.
12. Barkunan SR, Bhanumathi V, Sethuram J. Smart sensor for automatic drip irrigation system for paddy cultivation. Comput Electr Eng. 2019;73:180–93.
13. Mane S, Das N, Singh G, Cosh M, Dong Y. Advancements in dielectric soil moisture sensor calibration: A comprehensive review of methods and techniques. Comput Electron Agric. 2024;218:108686.
14. Almeida EL, Teixeira AS, Silva FC, Assis Júnior RN, Leão RAO. Método do papel-filtro Para obter a curva de retenção de água no solo. Rev Bras Cienc Solo. 2015;39(5):1344–52.
15. Novák V, Hlaváčiková H. Soil-Water retention curve. Applied soil hydrology theory and applications of transport in porous media. In V. Novák & H. Hlaváčiková (Eds.). Cham: Springer; 2019. pp. 77–96.
16. Ding X, El-Zein A. Predicting soil water retention curves using machine learning: A study of model architecture and input variables. Eng Appl Artif Intell. 2024;133:108122.
17. Menezes AS, Alencar TL, Assis Júnior RN, Toma RS, Romero RE, Costa MCG, Cooper M, Mota JCA. Functionality of the porous network of Bt horizons of soils with and without cohesive character. Geoderma. 2018;313:290–7.
18. Nascimento ÍV, Assis Júnior RN, Araújo JC, Alencar TL, Freire AG, Lobato MGR, Silva CP, Mota JCA. Nascimento CD V. Estimation of Van Genuchten equation parameters in laboratory and through inverse modeling with Hydrus-1D. J Agric Sci. 2018;10(3):102.
19. Šimůnek J, van Genuchten MT, Šejna M. Recent developments and applications of the HYSDRUS computer software packages. Vadose Zone J. 2016;15(7). pp. 1-25.
20. van Genuchten MT. A Closed-form equation for predicting the hydraulic conductivity of unsaturated soils. Soil Sci Soc Am J. 1980;44(5):892–8.
21. Freire AG, Alencar TLD, Chaves AF, Nascimento ÍVD, Assis RND, van Lier QDJ, Mota JCA. Comparison of devices for measuring soil matric potential and effects on soil hydraulic functions and related parameters. Agric Water Manag. 2018;209. pp. 134-141.
22. Costa TGA. Estimativa dos parâmetros da equação de van Genuchten com dados de umidade do solo e modelagem inversa com Hydrus-1D [Dissertation]. [Fortaleza]: Federal University of Ceará; 2019.
23. Hillel D, Krentos VD, Stylianou Y. Procedure and test of an internal drainage method for measuring soil hydraulic characteristics in situ. Soil Sci. 1972;114(5):395–400.
24. Wang L, Li XG, Guan ZH, Jia B, Turner NC, Li FM. The effects of plastic-film mulch on the grain yield and root biomass of maize vary with cultivar in a cold semiarid environment. Field Crops Res. 2018;216:89–99.
25. Blake GR, Hartge KH. Bulk density. In: Klute A, editor. Methods of soil analysis: part 1 physical and mineralogical methods. 2nd ed. Madison: Soil Science Society of America; 1986. pp. 363–75.
26. Blake GR, Hartge KH. Particle density. In: Klute A, editor. Methods of soil analysis: part 1 physical and mineralogical methods. 2nd ed. Madison: Soil Science Society of America; 1986. pp. 377–82.
27. Klute A. Water retention: laboratory methods. In: Klute A, editor. Methods of soil analysis: part 1 physical and mineralogical methods. 2nd ed. Madison: Soil Science Society of America; 1986. pp. 635–62.
28. Dourado-Neto D, Nielsen DR, Hopmans JW, Reichardt K, Bacchi OOS. Software to model soil water retention curves (SWRC, version 2.00). Sci Agric. 2000;57(1):191–2.
29. Mualem Y. A new model for predicting the hydraulic conduc. Water Resour Res. 1976;12(3):513–22.
30. Han XW, Shao MA, Horton R. Estimating Van Genuchten model parameters of undisturbed soils using an integral method. Pedosphere. 2010;20(1):55–62.
31. Hopmans JW, Šimůnek J, Romano N, Durner W. Inverse methods. In: Dane JH, Topp G, editors. Methods of soil analysis: part 4 - Physical methods. Madison: American Society of Agronomy, Soil Science Society of America; 2002. pp. 963–1008.
32. Marquardt DW. An algorithm for Least-Squares Estimation of nonlinear parameters. J Soc Ind Appl Math. 1963;11(2):431–41.
33. Nash JE, Sutcliffe JV. River flow forecasting through conceptual models part I - A discussion of principles. J Hydrol (Amst). 1970;10(3):282–90.
34. Machado RE, Vetorazzi CA, Xavier AC. Simulação de cenários alternativos de Uso Da Terra Em Uma microbacia utilizando técnicas de modelagem e Geoprocessamento. Rev Bras Cienc Solo. 2003;27(4):727–33.
35. ASCE. Criteria for evaluation of watershed models of the watershed management committee. Irrig Drain Div. 1993;119(3):429–42.
36. Lamontagne JR, Barber CA, Vogel RM. Improved estimators of model performance efficiency for skewed hydrologic data. Water Resour Res. 2020;56(9).e2020WR027101.
37. Jorge RF, Corá JE, Barbosa JC. Número mínimo de tensões Para determinação Da curva característica de retenção de água de Um Latossolo Vermelho eutrófico Sob sistema de semeadura Direta. Rev Bras Cienc Solo. 2010;34(6):1831–40.
38. Mota JCA, dos Santos EB, Queiroz A, dos S, Ferreira OP, de Souza Filho AG, Fregolente LG, da Silva FG, Pereira AP, de Sousa A, de Costa HH, do Nascimento MCG. Cashew residue Biochar enhances the pore network of cohesive soil in the Brazilian coastal tablelands. Geoderma Reg. 2025;42:e00979.
39. Alencar TL, Chaves AF, Freire AG, Nascimento ÍV, Queiroz AS, Mota JCA. Field capacity: methodological approach by static and dynamic criteria. Geoderma. 2019;353. pp. 81-88.
40. Ghiberto PJ, Moraes SO. Comparação de métodos de determinação Da condutividade hidráulica Em Um Latossolo Vermelho-Amarelo. Rev Bras Cienc Solo. 2011;35(4):1177–88.

41. Spasić M, Vacek O, Vejvodová K, Tejnecký V, Polák F, Borůvka L, Drábek O. Determination of physical properties of undisturbed soil samples according to V. Novák. MethodsX. 2023;10:102133.
42. van Lier QJ, Pinheiro EAR. An alert regarding a common misinterpretation of the Van Genuchten α parameter. Rev Bras Cienc Solo. 2018;42(0). e0170343.
43. Darmann F, Schwaighofer I, Kumpan M, Weninger T, Strauss P. New hydro-pedotransfer functions for Austrian soil mapping applications. Geoderma Reg. 2024;39:e00875.
44. Basile A, Ciollaro G, Coppola A. Hysteresis in soil water characteristics as a key to interpreting comparisons of laboratory and field measured hydraulic properties. Water Resour Res. 2003;39(12):1–12.
45. Guerra A, Nicolas F, Peddinti S, Ogunmokun F, Kisekka I. Evaluating a novel radio Frequency-Based soil moisture sensor under saline and imperfect installation. J Nat Resour Agric Ecosyst. 2024;2(3):119–28.

Publisher's note